

ORIGINAL ARTICLES

Feasibility of reproducible vendor independent estimation of cardiac function based on first generation speckle tracking echocardiography

Hanan Khamis¹, Sara Shimoni², Andreas Hagendorff^{3, 4}, Nahum Smirin¹, Zvi Friedman⁵, Dan Adam¹

1. Dept. of Biomedical Engineering, Technion-IIT, Haifa, Israel. 2. Non-invasive Cardiology Unit, Kaplan Medical Center, Rehovot, Israel. 3. Dept. of Cardiology-Angiology, University of Leipzig, Leipzig, Germany. 4. LIFE-Leipzig Research Center for Civilization Diseases, University of Leipzig, Leipzig, Germany. 5. GE Healthcare, Haifa, Israel.

Correspondence: Prof. Dan Adam. Address: Dept. of Biomedical Engineering, Technion-Israel Institute of Technology, Haifa, 32000 Israel. Email: dan@bm.technion.ac.il

Received: November 23, 2015

Accepted: December 20, 2015

Online Published: December 27, 2015

DOI: 10.5430/jbei.v2n2p57

URL: <http://dx.doi.org/10.5430/jbei.v2n2p57>

Abstract

Background: The clinical approval of speckle tracking echocardiography (STE) as an accepted measure of myocardial strain and of LV function is hindered by the discordance of the results among the vendors. Since echocardiography images are noisy, the measured displacements are smoothed or regularized, an operation affecting the strain results. We introduce an “Error-dependent weighted speckle tracking” (EWST) algorithm that allows sensitivity analysis to the different operations affecting noise and accuracy. The aim here was to study whether by modifying the properties of the post block-matching weighted smoothing in the EWST algorithm it was possible to assess the expected inter-vendor strain differences.

Methods and results: Forty-eight echocardiographic clips generated by a software-based phantom were used as “gold standard” for validation of the EWST algorithm. Also, a cohort of 435 normal subjects and a cohort of 47 patients, scanned/re-scanned at 2 frame-rates (~70; ~35), were studied using the EWST. The results were compared to those produced by a commercial product of a leading manufacturer (STE_{LV}). Peak global longitudinal strains [PRLS, (%)] and peak regional longitudinal strains [PRLS, (%)] were calculated and compared. Sensitivity to the region (ROI) determination was tested by shifting the apical endocardial boundary. The differences between the measured PGLS and the ground truth produced by the software-based phantom (average ± standard deviation) were 0.4% ± 0.6% and 1.0% ± 0.7% for the EWST and STE_{LV}, respectively. Normal values were calculated for 435 subjects: -18.82% ± 2.45%, -20.2% ± 5.6%, -19.62% ± 3.62%, 18.77% ± 4.31% by the EWST, and -21.24% ± 2.91%, -26.5% ± 5.0%, -21.1% ± 3.7%, -18.0% ± 3.9%, by the STE_{LV}, respectively, for the PGLS, the peak longitudinal apical, mid-ventricle and basal regions, respectively. A low bias, but significant, was found between PGLS, when calculated for the cohort of 47 patients scanned/re-scanned at 2 frame-rates: -0.80% ± 2.61% and -1.66% ± 2.66% for the EWST and STE_{LV}, respectively. When the apex location (and thus the ROI) was shifted, the bias (mm) (average ± standard deviation) relative to the default position was: 0.82 ± 1.04; 0.61 ± 0.72; -1.06 ± 0.75; and -1.87 ± 0.72, for displacement of 5 cm, 2.5 cm, -2.5 cm, and -5 cm, respectively, for the STE_{LV}. The EWST proved similarly sensitive to the shifting of the apex location.

Conclusions: STE is sensitive to the characteristics and amount of smoothing, as well as to the ROI positioning. Modification of the smoothing can produce different strain results, and different distribution of the regional strains. Thus it is preferable to use automatic determination of the ROI and methods that employ minimal smoothing or regularization.

Key words

Echocardiography, Strain imaging, Speckle decorrelation, Longitudinal strain, Block matching

1 Introduction

Two-dimensional (2-D) speckle tracking echocardiography (STE) software is nowadays offered by most vendors of echocardiography systems. The issue of inter-vendor variability raised the concern of many^[1-3], and caused the creation of the EACVI-ASE-Industry Strain Standardization Initiative^[4]. The primary source of discordance in the strain measurements among the vendors has been identified as the different post-processing algorithms, which smooth the raw displacement measurements that are based on speckle tracking^[5]. The different smoothing/processing approaches applied to the measurements, based on speckle tracking, may also explain the different myocardial strain values obtained by three-dimensional versus two-dimensional speckle-tracking echocardiography systems^[6]. The EACVI-ASE-Industry Strain Standardization Initiative produced some positive results, as one major vendor modified the post-processing software so that the STE results are of higher concordance with the other major vendor^[7].

Table 1. Acronyms and definitions

STE	Speckle tracking echocardiography
SAD	Sum of absolute differences
PGLS	Peak global longitudinal strain
PRLS	Peak regional longitudinal strain
HFR	High frame rate (scans of around 70 frames per second)
LFR	Low frame rate (re-scans at about half the HFR)
ROI	Region of interest
ROS	Region of search
LV	Left ventricle
2CH	2 chambers long axis cross-section
4CH	4 chambers long axis cross-section
APLAX	Apical long axis cross-section
TP	Tracking point
knot	Center of mass
TQ	Tracking quality
LUI	Local uniformity index
EWST	Error-dependent weighted speckle tracking algorithm
EWST w/10	Error-dependent weighted speckle tracking algorithm, with weights divided by 10
STE _{LV}	Speckle tracking software, by a leading vendor
SD	Standard deviation
basal region	Includes the 6 basal segments (anterior, anteroseptal, inferoseptal, inferior, inferolateral, anterolateral)
mid region	Includes the 6 mid segments (anterior, anteroseptal, inferoseptal, inferior, inferolateral, anterolateral)
apex region	Includes the 5 apex segments (anterior, septal, inferior, lateral, apex)

STE is based on tracking speckle patterns in conventional B-mode images, which is now feasible using readily available computational resources. Yet, in spite of its popularity, attested by thousands of clinical echocardiographic studies^[8-13] over the last 10 years, translating STE into the daily clinical routine is far more challenging in both the single and multi-vendor clinical environments. Thus, though the Strain Standardization Initiative reduced significantly the inter-vendor variability of the strain measurements, a consequent study^[14] concludes that current vendor independent STE

software does not reduce inter-vendor variability to a clinically acceptable level, and thus the same ultrasound machine and the same STE software should be used to measure Global strain in longitudinal and cross-sectional studies.

The present study, addresses the problem from a more basic point of view, analyzing the principles and specific details of the first generation STE algorithms, currently employed by the commercial vendors, with far reaching consequences. STE usually starts with the crucial step of segmenting the image, so as to define a region of interest (ROI), in which tracking is performed. This ROI is then readjusted from frame to frame as part of the tracking procedure. The ROI is further divided into a number of, usually overlapping, blocks, and the tracking is accomplished by a frame to frame block matching procedure, in which for each block (kernel) in a given frame - the most similar image block (kernel) is searched for in the consecutive frame. The tracking procedure employed by the first generation STE commercial products is a sequential two stage process. In the first stage, all kernels are individually matched unconstrained. This often results in a “non-physiologically” noisy displacement field, as illustrated in Figure 1, resulting from noise sources detailed below. The second stage usually consists of some weighted smoothing of the “noisy” displacement field, with displacements estimated to be more “reliable” given higher weights^[15, 16]. The two stage approach is often made as a compromise in order to save computational resources. The quality of the results strongly depends upon the characteristics of the imagery, which will affect the quality and stability of the speckle patterns, as well as on the details of the various algorithms.

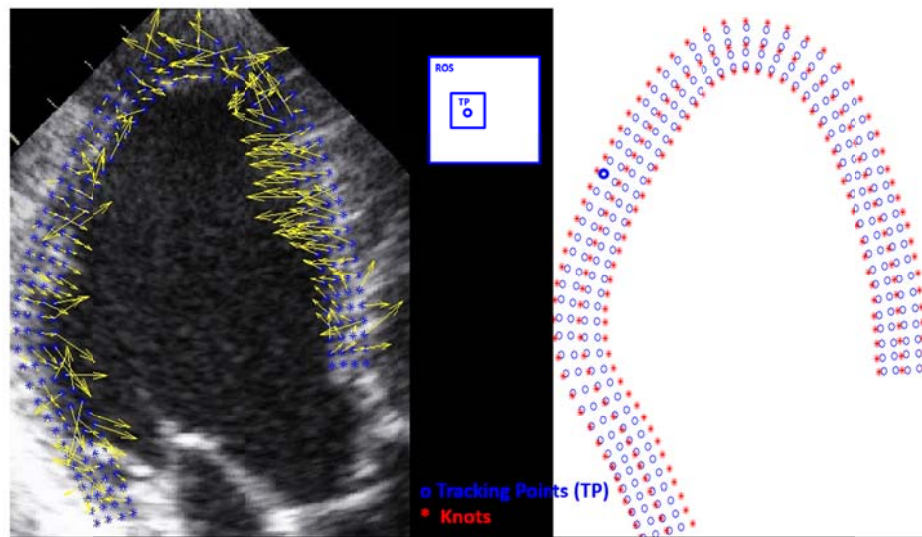


Figure 1. The geometric relationship between the TP and the knots, and their superposition within the predefined ROI. Each knot is located at the “center of gravity” of 20 TPs. (Left): The knots along the centerline of the LV wall are depicted, with their associated velocity vector, on an echocardiographic frame. (Right and blowup): Each set of 4 TP (small blue circles) is located across the myocardial width between the 3 knots (large red stars); (Middle): The ROS defined for each TP from one frame to the next, and the reduction of its size, based on more reliable TP displacement information. TP - tracking points.

Since speckles arise because sub-resolution scatterers cause interference patterns in the ultrasound image, the observed speckle pattern in most cases does not correspond to the underlying structure of the tissue^[17]. The speckle pattern is deterministic, but will gradually change when the structure is deformed or when the angle between the structure and the local wave-front changes^[18]. These result in variations in the speckle patterns, often referred to as speckle decorrelation noise. As long as these changes are small, the local motion of material points between two frames can be estimated by tracking of the speckle patterns in the images. This is what is often referred to as speckle tracking.

Speckle tracking is mostly performed by block-matching^[19-22], where the displacement of a material point is estimated by searching for the “best match” between a block in the source frame and a block in the target frame. The center of the block in the source frame is usually defined as a “tracking point” (TP)^[23]. The displacement search is usually limited to a region of search (ROS) around the TP, based on an estimation of the maximal tissue velocities.

Blocks are optimally matched when the cross correlation between the intensities of the respective pixels within the blocks is maximized. Since cross-correlation is relatively computationally intensive, an essentially equivalent criterion is commonly utilized - of minimizing the sum of absolute differences (SAD) between the pixels in the two images. Since to a certain degree speckle decorrelation noise is always present, the displacement that minimizes the SAD does not always yield the true displacement. Therefore, block matching based on speckle tracking always requires good image quality, as well as a certain minimal number of frames per heart cycle, so that noise level will be at a reasonably small level. It is also intuitively evident that speckle decorrelation noise will increase as the search region increases.

In order to allow reasonably accurate block matching, and thus reliable strain measurements, a second stage is commonly performed, following the block matching - smoothing, or regularization of the results^[24, 25]. The two stage approach employed by most commercial vendors, although inaccurate in principle from a theoretical perspective, is reasonable in cases with sufficiently low speckle decorrelation noise, namely: high frame rates, small regions of search and very good image quality. In these cases the number of outlying displacements is relatively small so that they could be practically eliminated using an appropriately weighted smoothing system, and also yield reasonably accurate strain values. Such smoothing, though, affects the overall results, modifying the results even in areas where there are no outliers. We hypothesize that the commercially available algorithms use some tradeoff between weighting and smoothing. The resulting strain values, therefore, most probably depend also on the details of the “weighted smoothing”, in addition to the dependencies on image quality, speckle decorrelation noise and the specific scanning parameters.

In order to study and better understand the accuracy and sensitivity of the strain measurements to various controlling parameters-which are proprietary information of the vendors, we developed a fully “open” generic algorithm and compare here its tracking and strain results in a software-based phantom and in a large cohort, to those obtained with the algorithm of a leading vendor (referred as STE_{LV}). The comparison between the two algorithms is done as function of the model’s weighting/smoothing parameter (termed N below), under the hypothesis that the various algorithms could be mimicked by properly varying one parameter (or for an extreme case - maybe two parameters) in our generic algorithm.

2 Generic open STE algorithm

An error-dependent weighted speckle tracking (EWST) algorithm has been developed as an open, generic algorithm, for the purpose of roughly assessing the differences in strain values resulting from using commercial codes. Here, the comparison is performed versus one vendor, one of the leading vendors which established this measure. It is hypothesized that the proprietary commercial codes mainly differ in the amount and the characteristics of the post block-matching weighted smoothing. It is thus suggested that changing the amount of smoothing/weighting, by modifying the parameter N (see below) in the EWST algorithm in various situations, may help assess the expected inter-vendor strain differences.

The EWST algorithm is primarily based on the method previously reported^[23, 26, 27]. The algorithm contains a single smoothing/weighting function, with one parameter N, which controls the amount of spatial smoothing. Briefly, the image is first segmented into two parts, separating the imaged left ventricular myocardial zone from the rest of the image. This defines a ROI, which is then being tracked from frame to frame. This process should be, and is automatic, in order to obtain reproducible strain results. In many echocardiographic clips, though, the apical region is rather noisy, which makes it difficult to view and detect the apical subendocardial boundary. This is usually caused by clutter noise, as well as the existence of trabeculae. As the separation of the usually higher strain trabecular zone from the lower strain compact

muscular zone^[28] is essential for accurate muscular strain estimation, the wall thickness at the apex was set in the EWST algorithm as half the septal wall thickness, determined by the thickness at the mid inferoseptal segment.

Three chains of points, knots^[23], are defined within the ROI, one imposed along the inner (subendocardial) boundary of the myocardium, one along the outer (subepicardial) boundary, and one along the line in between (mid wall). The 3 chains of knots are assumed to be along 3 smooth curves and are further assumed to mark the same physical points at all frames. This last assumption is also dependent on the assumption of negligible out-of-plane motion, which may not hold well at the apical and basal areas, due to the LV rotation. Each knot is then surrounded by a set of TPs, each representing a tracking block, which is a square area of the image. The knot-TP structure is depicted in Figure 1. As mentioned above, the displacement of each TP from one frame to the next is computed using a minimum SAD algorithm, searched within a region of search (ROS), which is, of course, within the ROI (see Figure 1).

Weighted smoothing: Following the description in our previous publication^[26], the displacement at each knot is computed by a 2 stage weighted smoothing scheme. First, the displacement field of the TP is smoothed using a weighted bilinear approximation. In the second stage, the displacements of all the knots, along the 3 chains are smoothed, using a smoothing spline, as detailed elsewhere^[23]. The open-source STE algorithm proposed here allows the operator, differently from previously reported algorithms, a control of the degree of the smoothing of the spline by defining a weighting-parameter N , which will effectively increase the amount of smoothing for noisy data. The weighting scheme is probably one of the more important details in the speckle tracking algorithm and is proprietary to all commercial vendors. Therefore, in order to be able to explore the dependence of the strain values on the details of the weighting scheme, an open generic STE algorithm has been developed as part of the present study. We will show below that strain values in general, and their distribution in the LV in particular, may be tailored using this scheme by varying the value of a single parameter. The strain distribution along the left ventricle (LV) can be either made to resemble the distribution obtained by cMRI^[29], as well as that of the pioneering works of the T. Arts group^[30,31], both claiming that the longitudinal strain is evenly distributed along the entire LV, or those obtained by the commercial vendors STE algorithms.

The weights of the TPs in the EWST algorithm are defined by their estimated relative displacement error σ . The displacement error is calculated as the normalized difference between the measured displacements, which is obtained by minimizing the SAD corresponding to the TP, and the “ground truth” displacement. Since the latter is unknown, it is estimated using the displacements within a defined neighborhood. The weights at each $(i, j)^{\text{th}}$ TP are then calculated as the inverse function of the resulted displacement error $w(i, j) = \frac{1}{N\sigma(i, j)^k}$. A high value of the parameter k would mean lower weightings to “outliers” (noise). Higher N would result in higher “spline smoothing” at the knots. In the present study we constricted ourselves to the choices $k = 1, N = 1$ and $k = 1, N = 10$. Thus, 2 sets of weights $w(i, j) = \frac{1}{\sigma(i, j)}$ (referred to below as EWST) and $w(i, j) = \frac{1}{10\sigma(i, j)}$ (referred to below as EWST w/10) have been studied. These parameters can be set by the operator prior to the analysis, thus controlling the smoothing degree.

3 Methods

3.1 Phantom validation

To validate 2-D motion tracking and test the limits of the EWST algorithm, a software-based phantom (custom-built by the lab of Prof. Jan D’hooge, from KU Leuven University Medical Center) generated four sets of apical 2-D sequences, including 4 levels of de-correlation noise. This data set was recommended by the EACVI and ASE to the commercial vendors as the “gold-standard” to be used in their efforts to standardize deformation imaging^[32]. A total of 48 clips have been generated, modeling the shape of the LV myocardial cross-section, simulating the following conditions:

- 1) Four different clinical cases:
 - Healthy myocardium - heart rate 73 bpm, frame rate 62 fps;
 - Dilated Cardiomyopathy (DCM) - heart rate 83 bpm, frame rate 62 fps;
 - Stress - heart rate 158 bpm, frame rate 84 fps;
 - Left Ventricular Hypertrophy (LVH) - heart rate 73 bpm, frame rate 62 fps;
- 2) Four noise levels (0%, 20%, 40% and 60%)
- 3) Three variations of de-correlation noise

Apical B-Mode image sequences (mimicking 2CH view) were used for validation and evaluation of the speckle tracking algorithms (EWST and STE_{LV}). In order to evaluate the noise-dependency and the accuracy of each software package, the maximal global strain values were computed and compared to the ground truth values provided by the software-based phantom.

3.2 Clinical data acquisition

Scanning was performed with either GE VIVID 7 or VIVIDq, with the standard 2.5 MHz cardiac probe. The study was approved by the IRB of Kaplan Hospital, Rehovot, Israel, and the IRB of the University of Leipzig, Leipzig, Germany. The patient records/information in each case was anonymized and de-identified prior to analysis.

Two groups of subjects have been scanned (see Table 2).

Table 2. The number and percent of clips included in each group of subjects

	Group 1 (435 subjects)		Group 2 (47 subjects)			
	Total of 1,305 clips	Percent	Global (total of 135 clips)	Basal LV level (out of total of 270 regions)	Mid LV level (out of total of 270 regions)	Apical LV level (out of total of 270 regions)
EWST	1,283	98.31%	135	229	260	251
EWST w/10	1,292	99.00%	135	246	265	255
STE _{LV}	1,290	98.85%	134	243	268	264

Note. Number and percent of clips included in the analysis of Group 1 (435 normal subjects), and the number of regions included in the analysis of Group 2 (clips that were acquired at both high frame-rate and low frame-rate). The acquisition included the 3 apical long axis views for each of the three different algorithms (EWST, EWST w/10 and STE_{LV}).

Group 1: 435 normal subjects (172 males, age 55 ± 12 years, mean BSA 1.85 ± 0.37), without any known cardiac disease, were scanned according to the regular clinical protocol, including the 3 standard apical views.

The data (a total of 1,305 clips - 2CH, 4CH and APLX views) was analyzed by the EWST algorithm, as well as by the STE_{LV} algorithm, and the EWST w/10 variant. The following values were calculated:

- 1) Peak global longitudinal strains [PGLS (%)], calculated as the average of strain in all 18 segments;
- 2) Peak regional longitudinal strains [PRLS (%)], for 3 regions - calculated as the average of strains in all the respective segments in the 3 apical views: basal region - includes the 6 basal segments; mid-ventricle region - includes the 6 mid segments; apex region - includes the 6 apical segments.

Both PGLS and PRLS are values widely used in clinical studies.

Group 2: 47 subjects (cardiac patients and normal subjects, 33 males, age 55 ± 14 years, mean LVEF $57\% \pm 5\%$) were scanned twice by the same sonographer: once at normal frame rate of ~ 70 frame per second, termed HFR below, and a second time at a low frame rate ~ 35 frames per second, termed LFR below. The scanning was performed according to the regular clinical protocol, including the 3 standard apical views.

The data (a total of 141 clips) was analyzed for the 2 different frame rates, HFR and LFR, by the EWST algorithm, as well as by the STE_{LV} algorithm, and the EWST w/10 (N = 10) variant. Both PGLS (%) and PRLS (%) were calculated as described above.

3.3 Speckle tracking analysis

3.3.1 Global and regional strains

PGLS (%) and PRLS (%) were assessed using the EWST, the STE_{LV} , and the EWST w/10 algorithms. The algorithms were all run automatically, with no operator intervention. Figure 2 depicts a typical example of PGLS and PRLS time curves calculated using: (A) EWST, (B) STE_{LV} , and (C) EWST w/10. It can be clearly noted that the resultant apical curves in both STE_{LV} , and EWST w/10, reach at systole very high strain values ($> 30\%$ and $> 28\%$, respectively), much higher than expected.

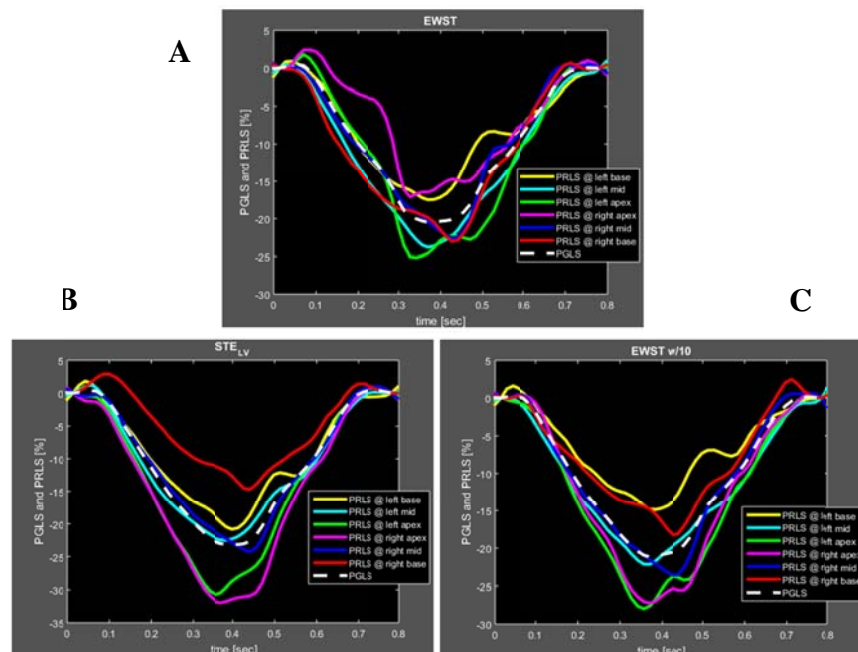


Figure 2. Typical PGLS and PRLS time curves calculated using: (A) EWST, (B) STE_{LV} , and (C) EWST w/10. In both STE_{LV} , and EWST w/10 the two apical curves reach at systole very high strain values ($>30\%$ and $>28\%$, respectively).

Since the apical endocardial boundary is sometimes relatively difficult to detect, even in high quality scans, the wall thickness at the apex was set in the EWST algorithm as half the septal wall thickness, determined by the thickness at the mid inferoseptal segment. This reduced width correlates well with MRI findings regarding the apical wall thickness as depicted in Figure 3.

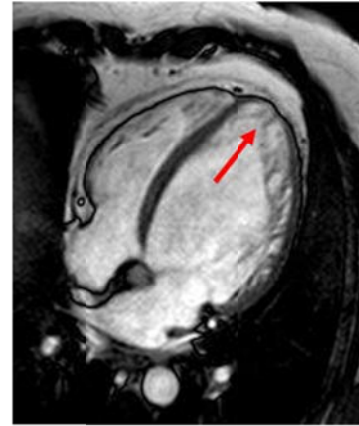


Figure 3. Cardiac-MRI image of the LV, exhibiting narrow wall thickness at the apex, as well as the trabeculae, which are specifically dense at the apex region.

3.3.2 Sensitivity to the ROI apical-subendocardial boundary

Data from 20 subjects was used for the study of the sensitivity of the PGLS (%) to the precise position of the ROI. Five different ROI positions were generated by vertically (axially) moving the most apical sub-endocardial border point relative to the default automatic position d (mm): d , $d \pm 2.5$, $d \pm 5$ (mm). The horizontal position was not changed. Whenever the apical sub-endocardial border point is shifted, the algorithm detects a new the endocardial border, and thus re-determines the ROI. Such changes may affect the tracking, and thus also the strain calculations.

3.3.3 Speckle tracking accuracy versus noise

In group 2, the measures used for comparison were, as above, the PGLS (%) and the PRLS (%). The differences between the results (of the 3 algorithms) at low and high frames rates were compared by the Bland Altman test.

3.3.4 Sensitivity to weighting parameters

The PGLS (%), as well as the PRLS (%) at the apical, mid-ventricle and basal segments, were compared when different weights were used. The data of 435 normal subjects, (Group 1) was used for this study.

3.4 Statistical analyses

Continuous data are expressed as mean \pm SD. The agreements between the results produced by the two algorithms, for the HFR and LFR scans were compared using the Bland-Altman analysis. Mean differences between STE_{LV} and EWST were tested using Student's t -test. $P < .01$ was considered to be significant.

4 Results

4.1 Validation using software-based phantom

The 48 clips generated by the software-based phantom, were used for validation of the algorithms. The PGLS calculated by the EWST was compared to the “ground truth” values imposed by the software-based phantom, and the average error for all clips was -0.4%. The results are shown in Figure 4A. The PGLS was also calculated by the STE_{LV} and compared to the ‘ground truth’ imposed by the software-based phantom; the average error in this case for all clips was 1.0%. The results are shown in Figure 4B. One can also note that while the measured results, as calculated by the EWST algorithm, are the same or somewhat smaller than the “ground truth”, the results calculated by the STE_{LV} algorithm are nearly always (except some runs of dilated cardiomyopathy) larger than the “ground truth”.

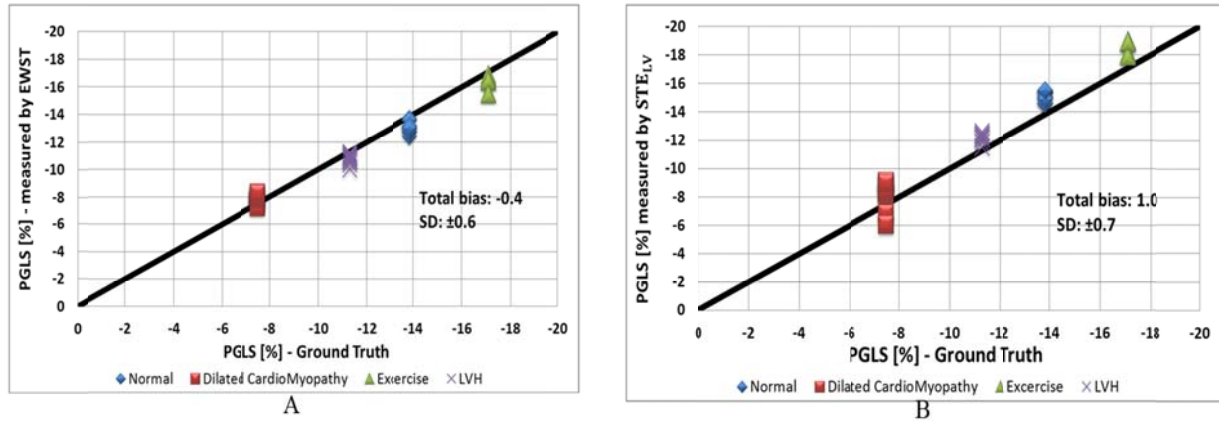


Figure 4. Results of the software-based phantom studies. Software-based phantom studies, modeling the shape changes of the LV myocardial cross-section, serving as the “ground truth” PGLS, are compared to those measured by the EWST algorithm (A), and the STE_{LV} (B). 48 clips have been generated, exhibiting 4 different clinical cases: Healthy myocardium, DCM, Stress and LVH, at 4 noise levels (0%, 20%, 40% and 60%), and 3 variations of de-correlation noise.

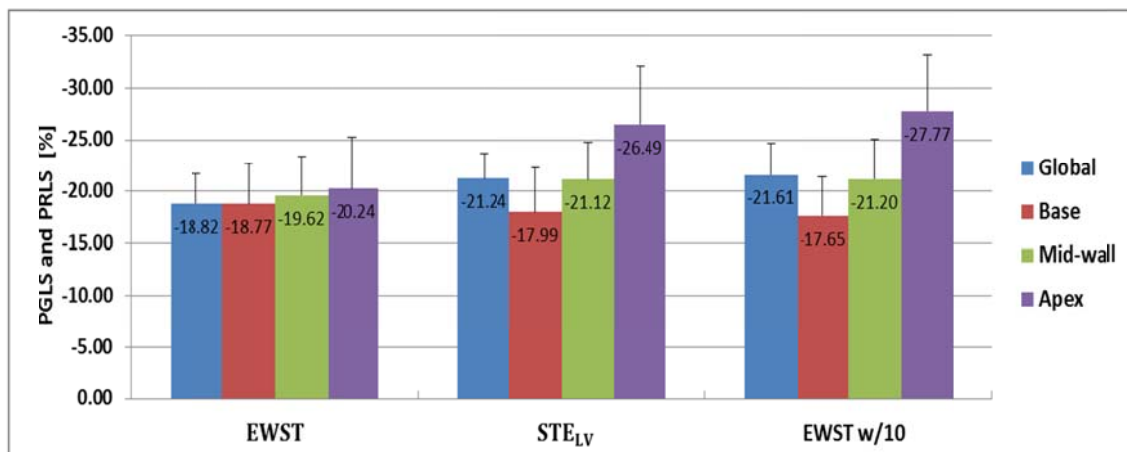


Figure 5. Peak Longitudinal Strain, calculated for the 435 normal subjects (Group 1) at base, mid-ventricle and apex regions of the LV (PRLS), and also the global values (PGLS), for the three algorithms (STE_{LV}, EWST and EWST-w/10).

4.2 Normal global and regional strain values (Group 1)

Tracking using an automatic ROI was feasible in 1,290 out of 1,305 (98.9%) clips for STE_{LV}, 1,283 (98.3%) for EWST and 1,292 (99.0%) for EWST w/10. Global and regional strain values were calculated and compared. The results are presented in Figure 5. As can be seen in this figure, the regional strains, as calculated by the EWST, are not significantly different from each other. On the other hand, the regional strains, as calculated by either STE_{LV} or EWST w/10, are significantly different. Typical PGLS and PRLS curves computed using the three variants are displayed in Figure 2.

A fair agreement was observed for the PGLS comparing STE_{LV} with EWST w/10 (bias = 0.2%, limits of agreement [LOA] = 2.7%, *P*-values are provided in Table 3). PRLS values at the mid-ventricular region, by STE_{LV} and the EWST w/10 were not significantly different, whereas at the base the strain values were slightly but still significantly different. Differences at the apex were all large and significant. However, both PGLS and PRLS values at all LV levels, as calculated by the EWST and by the STE_{LV} algorithms, were all significantly different (see Table 3).

Table 3. Comparison of bias and standard deviation between the PGLS (%) and PRLS (%) values

Algorithms being compared		Bias	SD (±)
Global	STE _{LV} -EWST	-2.66*	1.60
	STE _{LV} -EWST w/10	0.20	1.34
Base	STE _{LV} -EWST	0.80*	2.61
	STE _{LV} -EWST w/10	-0.32*	1.95
Mid-ventricle	STE _{LV} -EWST	-1.53*	2.40
	STE _{LV} -EWST w/10	0.04	1.71
Apex	STE _{LV} -EWST	-6.33*	4.76
	STE _{LV} -EWST w/10	-2.91*	5.87

Note. Comparison of bias and standard deviation between the PGLS (%) and PRLS (%) values obtained by the different algorithms-STE_{LV}, EWST, and EWST w/10 in the cohort of 435 normal subjects. P-values of two-tailed paired T-Test are also presented (*Significance $P < .01$). Significant differences were found in all regions between EWST vs. STE_{LV}, and between STE_{LV} and EWST w/10 only at the basal and apical regions.

4.3 Speckle tracking accuracy versus noise (Group 2)

Of group 2, two sets of 135 clips, one measured at HFR and the other at LFR (out of 141 each), were analyzed. 6 clips were excluded due to poor image quality. In addition, segments with bad tracking quality were excluded as detailed in Table 2 below.

The biases in PGLS and in PRLS between the two sets of HFR and LFR clips, for the 3 variants EWST, EWST w/10, and STE_{LV}, are listed in Table 4. Interestingly, PGLS values for HFR clips are consistently higher (more negative) than those for LFR clips by all 3 algorithms. The PGLS is also significantly different when comparing the HFR and LFR clips for all 3 software versions ($P < .01$). The standard deviation (SD) of all variants was about 4.15% on average.

Table 4. Comparison of bias and standard deviation PGLS (%) and PRLS (%), between the two sets of high frame-rate and low frame-rate clips

	EWST			EWST w/10			STE _{LV}		
	mean	SD	P-value	mean	SD	P-value	mean	SD	P-value
Global	-0.80%	2.61%	<< .001*	-0.74%	3.07%	.0057*	-1.66%	2.66%	<< .001*
Base	-0.28%	4.42%	.347	-0.57%	3.72%	.080	-1.46%	4.28%	<< .001*
Mid-ventricle	-0.31%	3.99%	.194	-0.63%	3.80%	.003*	-2.07%	3.88%	<< .001*
Apex	-0.94%	5.94%	< .010*	-0.74%	5.70%	.037	-1.39%	5.54%	<< .001*

Note. Comparison of bias and standard deviation between the two sets of high frame-rate and low frame-rate clips, in terms of PGLS (%) and PRLS(%), for each of the 3 algorithm (the EWST with 2 variants, and the STE_{LV}). P-values of two-tailed paired t-Test are also presented (*Significance $P < .01$).

4.4 Speckle tracking sensitivity to the ROI position

Data from 20 subjects was analyzed. The general trend for all 3 algorithms was increased strain values (strains became more negative), once the ROI was shifted from that determined automatically.

The PGLS values are significantly different among all comparisons ($P < .01$), except for at the 2 uppermost positions d+2.5 and d+5 (mm) ($P = .402$). The averaged bias [d- (d+ displacement)] and standard deviation relative to the default position d were: d+5 vs. d: 0.82 ± 1.04 ; d+2.5 vs. d: 0.61 ± 0.72 ; d-2.5 vs. d: -1.06 ± 0.75 ; d-5 vs. d: -1.87 ± 0.72 . The PGLS decreases for positions above the default and increases for shifts to the other direction. These results are provided for the STE_{LV}, but were very similar for the EWST and EWST w/10 algorithms.

5 Discussions

We have introduced a new “open” generic STE algorithm, EWST, following the hypothesis that variations in one of its parameters that control the amount of spatial smoothing would roughly represent the different STE packages by the various vendors.

The EWST algorithm was first validated by applying it to the software-based phantom generated in the lab of Prof. Jan D’hooge, from K.U. Leuven University Medical Center. The average and standard deviation of the differences between the PGLS as measured by EWST algorithm and the ground truth, generated by the software-based phantom, were found superior to those of a leading industry vendor (STE_{LV}).

Our results indicate that reproducibility of regional or even global longitudinal strain is challenging even with the same scanner and the same STE software. The high sensitivity of the strain results to the ROI position, especially in the apical region, seems to require exceptionally high image quality. This very often presents a challenge, as a result of near field clutter. This high sensitivity to the position of the subendocardial apical point may be attributed to the high concentration of trabeculae at this area^[28]. This highly complex apical structure may be observed with cMRI (see Figure 3), and may now also be observed when employing recently introduced premium ultrasound scanners. We have also shown that strain results depend on acquisition parameters such as frame rate to heart rate ratios, and that these dependences are algorithm specific. It is perhaps not surprising that these dependences are most predominant in the apical regions. Although the STE_{LV} and the 2 EWST versions were in reasonable agreements with the “ground truth” global strain values of the Leuven model, there were differences between the two algorithms when the global and regional strains of 435 normal subjects were compared. STE_{LV} correlated better with EWST w/10, in which the spatial smoothing is significantly increased relative to that in the EWST. Since the same scans and the same ROI have been used for all 3 algorithm versions, we could separate the effects of changes in the algorithm from the effects of the changes in the ROI or in the scanning parameters. We hypothesize that the EACVI-ASE-Industry Strain Standardization Initiative, *i.e.* decreasing the discordance among the vendors, can be simulated by our changing the parameter N of our EWST generic algorithm.

Yet, the algorithm that uses minimal smoothing, the EWST, produces results less affected by mathematical processing, thus is assumed to be more accurate. It should be noted that although we can bring the EWST algorithm to a high level of agreement with *e.g.* the STE_{LV} , this does not mean that either of them yields the “true” strain values. In fact, the strain values and their regional distribution as calculated by the EWST are regionally more uniform and closer to those by cMRI^[29].

To the best of our knowledge, we are the first to study the consistent error, which is a direct result of the fact that block matching and smoothing are separated into two consecutive stages. We found by comparing global and regional strain values for clips scanned at different “frame rate to heart rate” ratios that for these types of algorithms, both global and regional strain values depend upon “frame rate to heart rate” ratios and that the dependences seem to be algorithm specific.

We have further shown that these kinds of algorithms yield neither the “true” values of global strain, nor the correct distribution of the regional strains along the left ventricle. In fact, higher smoothing (larger values of N in our EWST model) results in higher (more negative) global strain values and higher regional strain non-uniformities (higher ratios of apical to basal strains). Thus, smoothing should be kept minimum, similar to the EWST with $N = 1$.

6 Conclusions

Strain values depend to various degrees on specific scan parameters, such as frame rate or line density even for the same scanner and STE software package, affecting accuracy and reproducibility. Strain values depend on image segmentation, mainly in the trabeculae-rich apical sub-endocardial regions. We are thus unsure as to the extent to which scans with

qualities that are inferior to those offered by the state of the art premium scanners, can be used for studying strains in a clinical setting.

Based on the limited comparison made here, between the EWST and a commercial product, one may conclude that first generation STE software packages that are separated into 2 consecutive stages (tracking then smoothing), as the one used here for the comparison, would suffer from inaccuracies and some uncertainties. Their results would depend on the degree of smoothing. One may also conclude that inter-vendor variability could be minimized by adjusting the smoothing parameters, based on sufficiently large patient cohorts. Future STE software should treat outliers (noise) differently, by eliminating them instead of smoothing them together with the uncorrupted data.

Acknowledgements

The authors are grateful to Prof. Jan D'hooge and his colleagues, from K.U. Leuven University Medical Center, for providing the software-based phantom data. This study was supported by the Technion R&D Fund for research.

References

- [1] Bansal M, Cho GY, Chan J, *et al.* Feasibility and accuracy of different techniques of two-dimensional speckle based strain and validation with harmonic phase magnetic resonance imaging. *J Am Soc Echocardiogr.* 2008; 21(12): 1318-25. PMID:19041575. <http://dx.doi.org/10.1016/j.echo.2008.09.021>
- [2] Yuda S, Sato Y, Abe K, *et al.* Inter-Vendor Variability of Left Ventricular Volumes and Strains Determined by Three-Dimensional Speckle Tracking Echocardiography. *Echocardiography.* 2014; 31(5): 597-604. PMID:25070187. <http://dx.doi.org/10.1111/echo.12432>
- [3] Gayat E, Ahmad H, Weinert L, *et al.* Reproducibility and inter-vendor variability of left ventricular deformation measurements by three-dimensional speckle-tracking echocardiography. *J Am Soc Echocardiogr.* 2011; 24(8): 878-85. PMID:21645991. <http://dx.doi.org/10.1016/j.echo.2011.04.016>
- [4] Thomas JD, Badano LP. EACVI-ASE-industry initiative to standardize deformation imaging: a brief update from the co-chairs. *European Heart Journal-Cardiovascular Imaging.* 2013; 14(11): 1039-40. PMID:24114804. <http://dx.doi.org/10.1093/ehjci/jet184>
- [5] Negishi K, Lucas S, Negishi T, *et al.* What is the primary source of discordance in strain measurement between vendors: imaging or analysis? *Ultrasound in Medicine & Biology.* 2013; 39(4): 714-20. PMID:23414723. <http://dx.doi.org/10.1016/j.ultrasmedbio.2012.11.021>
- [6] Muraru D, Cucchini U, Mihăilă S, *et al.* Left ventricular myocardial strain by three-dimensional speckle-tracking echocardiography in healthy subjects: reference values and analysis of their physiologic and technical determinants. *Journal of the American Society of Echocardiography.* 2014; 27(8): 858-71. PMID:24975996. <http://dx.doi.org/10.1016/j.echo.2014.05.010>
- [7] Yang H, Fukuda N, Marwick T, *et al.* Improvement in Strain Concordance between the Vendors after Strain Standardization Initiative. *Journal of the American College of Cardiology.* 2014; 63(12_S). [http://dx.doi.org/10.1016/S0735-1097\(14\)61125-6](http://dx.doi.org/10.1016/S0735-1097(14)61125-6)
- [8] D'hooge J, Konofagou E, Jamal F, *et al.* Two-dimensional ultrasonic strain rate measurement of the human heart in vivo. *IEEE Transactions on Ultrasonics, Ferroelectrics and Frequency Control.* 2002; 49(2): 281-6. <http://dx.doi.org/10.1109/58.985712>
- [9] Leitman M, Lysyansky P, Sidenko S, *et al.* Two-dimensional strain-a novel software for real-time quantitative echocardiographic assessment of myocardial function. *Journal of the American Society of Echocardiography.* 2004; 17(10): 1021-29. PMID:15452466. <http://dx.doi.org/10.1016/j.echo.2004.06.019>
- [10] Sutherland GR, Di Salvo G, Claus P, *et al.* Strain and strain rate imaging: a new clinical approach to quantifying regional myocardial function. *Journal of the American Society of Echocardiography.* 2004; 17: 788-802. PMID:15220909. <http://dx.doi.org/10.1016/j.echo.2004.03.027>
- [11] Jenkins C, Bricknell K, Hanekom L, *et al.* Reproducibility and accuracy of echocardiographic measurements of left ventricular parameters using real-time three-dimensional echocardiography. *J Am Coll Cardiol.* 2004; 44(4): 878-86. PMID:15312875. <http://dx.doi.org/10.1016/j.jacc.2004.05.050>
- [12] Singh GK, Cupps B, Pasque M, *et al.* Accuracy and reproducibility of strain by speckle tracking in pediatric subjects with normal heart and single ventricular physiology: a two-dimensional speckle-tracking echocardiography and magnetic resonance imaging correlative study. *Journal of the American Society of Echocardiography.* 2010; 23(11): 1143-52. PMID:20850945. <http://dx.doi.org/10.1016/j.echo.2010.08.010>

- [13] Jasaityte R, Heyde B, D'hooge J. Current State of Three-Dimensional Myocardial Strain Estimation Using Echocardiography. *Journal of the American Society of Echocardiography*. 2013; 26: 15-28. PMID:23149303. <http://dx.doi.org/10.1016/j.echo.2012.10.005>
- [14] Nagata Y, Takeuchi M, Mizukoshi K, *et al.* Intervendor Variability of Two-Dimensional Strain Using Vendor-Specific and Vendor-Independent Software. *J Am Soc Echocardiogr*. 2015; 28: 630-41. PMID:25747915. <http://dx.doi.org/10.1016/j.echo.2015.01.021>
- [15] De Craene M, Piella G, Camara O, *et al.* Temporal diffeomorphic free-form deformation: Application to motion and strain estimation from 3D echocardiography. *Medical Image Analysis*. 2012; 16(2): 427-50. PMID:22137545. <http://dx.doi.org/10.1016/j.media.2011.10.006>
- [16] Jasaityte R, Heyde B, D'hooge J. Current state of three-dimensional myocardial strain estimation using echocardiography. *Journal of the American Society of Echocardiography*. 2013; 26(1): 15-28. PMID:23149303. <http://dx.doi.org/10.1016/j.echo.2012.10.005>
- [17] Anderson ME, Soo MS, Trahey GE. In vivo breast tissue backscatter measurements with 7.5- and 10-MHz transducers. *Ultrasound in Medicine and Biology*. 2001; 27(1): 75-81. [http://dx.doi.org/10.1016/S0301-5629\(00\)00310-0](http://dx.doi.org/10.1016/S0301-5629(00)00310-0)
- [18] Meunier J. Tissue motion assessment from 3D echographic speckle tracking. *Physics in Medicine and biology*. 1998; 43(5): 1241-54. PMID:9623653. <http://dx.doi.org/10.1088/0031-9155/43/5/014>
- [19] Bamber CJ, Bush LN. Freehand elasticity imaging using speckle decorrelation rate. *IEEE Symposium on Acoustical Imaging* (Eds P. Tortoli and L. Masotti). 1996; 22: 285-92. http://dx.doi.org/10.1007/978-1-4419-8772-3_45
- [20] Bohs LN, Geiman BJ, Anderson ME, *et al.* Ensemble tracking for 2D vector velocity measurement: Experimental and initial clinical results. *IEEE Transactions on Ultrasonics, Ferroelectrics and Frequency Control*. 1998; 45(4): 912-24. PMID:18244246. <http://dx.doi.org/10.1109/58.710557>
- [21] Zhu Y, Hall TJ. A modified block matching method for real-time freehand strain imaging. *Ultrasonic Imaging*. 2002; 24(3): 161-176. PMID:12503771. <http://dx.doi.org/10.1177/016173460202400303>
- [22] Li PC, Lee WN. An efficient speckle tracking algorithm for ultrasonic imaging. *Ultrasonic imaging*. 2002; 24(4): 215-28. <http://dx.doi.org/10.1177/016173460202400402>
- [23] Lysiansky M, Bachner-Hinenzon N, Khamis H, *et al.* Measurements of transmural strain variations by two dimensional ultrasound speckle tracking. *Journal of Biomedical Graphics and Computing*. 2012; 2(1): 15-30. <http://dx.doi.org/10.5430/jbge.v2n1p15>
- [24] Sun Q, Hossack JA, Tang J, *et al.* Speckle reducing anisotropic diffusion for 3D ultrasound images. *Computerized Medical Imaging and Graphics*. 2004; 28(8): 461-70. PMID:15541953. <http://dx.doi.org/10.1016/j.compmedimag.2004.08.001>
- [25] Zhang F, Yoo YM, Mong KL, *et al.* Nonlinear diffusion in Laplacian pyramid domain for ultrasonic speckle reduction. *IEEE Transactions on Medical Imaging*. 2007; 26(2): 200-11. PMID:17304734. <http://dx.doi.org/10.1109/TMI.2006.889735>
- [26] Rappaport D, Adam D, Lysyansky P, *et al.* Assessment of myocardial regional strain and strain rate by tissue tracking in B-mode echocardiograms. *Ultrasound in Med. & Biol*. 2006; 32(8): 1181-92. PMID:16875953. <http://dx.doi.org/10.1016/j.ultrasmedbio.2006.05.005>
- [27] Rappaport D, Konyukhov E, Adam D, *et al.* In-vivo validation of a novel method for regional myocardial wall motion analysis based on Echocardiographic Tissue Tracking. *Med. Bio. Eng. Comput*. 2008; 46: 131-7. PMID:17985167. <http://dx.doi.org/10.1007/s11517-007-0281-z>
- [28] Peters DC, Ennis DB, McVeigh ER. High-resolution MRI of cardiac function with projection reconstruction and steady-state free precession. *Magnetic Resonance in Medicine*. 2002; 48(1): 82-8. PMID:12111934. <http://dx.doi.org/10.1002/mrm.10193>
- [29] Edvardsen T, Gerber BL, Garot J, *et al.* Quantitative assessment of intrinsic regional myocardial deformation by Doppler strain rate echocardiography in humans validation against three-dimensional tagged magnetic resonance imaging. *Circulation*. 2002; 106(1): 50-6. PMID:12093769. <http://dx.doi.org/10.1161/01.CIR.0000019907.77526.75>
- [30] Arts T, Meerbaum S, Reneman RS, *et al.* Torsion of the left ventricle during the ejection phase in the intact dog. *Cardiovascular Research*. 1984; 18(3): 183-93. <http://dx.doi.org/10.1093/cvr/18.3.183>
- [31] Prinzen FW, Arts T, Van der Vusse GJ, *et al.* Fiber shortening in the inner layers of the left ventricular wall as assessed from epicardial deformation during normoxia and ischemia. *J Biomech*. 1984; 17: 801-12. [http://dx.doi.org/10.1016/0021-9290\(84\)90111-8](http://dx.doi.org/10.1016/0021-9290(84)90111-8)
- [32] Thomas JD, Badano LP. EACVI-ASE-industry initiative to standardize deformation imaging: a brief update from the co-chairs. *European Heart Journal-Cardiovascular Imaging*. 2013; 14(11): 1039-40. PMID:24114804. <http://dx.doi.org/10.1093/ehjci/jet184>